To the Graduate Council:

I am submitting herewith a thesis written by Daniel L. Sutliff entitled, "Design of a Laser Welding Nozzle Incorporating an Aerodynamic Window for Laser Beam Delivery Optics Protection." I have examined the final copy of this thesis for form and content and recommend that it be accepted in partial fulfillment of the requirements for the degree of Master of Science, with a Major in Aerospace Engineering.

T. Dwayne McCay
T. Dwayne McCay, Major Professor

We have read this thesis
and recommend its acceptance:

Mary Helen McCay

Roger A. Crawford

Accepted for the Council:

Cwminkel
Vice Provost
and Dean of the Graduate School

STATEMENT OF PERMISSION TO USE

In presenting this thesis in partial fulfillment of the requirements for a Masters degree at the University of Tennessee, Knoxville, I agree that the Library shall make it available to borrowers under the rules of the library. Brief quotations from this thesis are allowable without special permission, provided that accurate acknowledgement of the source is made.

Permission for extensive quotation from or reproduction of this thesis may be granted by my major professor, or in his absence, by the Head of Interlibrary Services when, in the opinion of either, the proposed use of the material is for scholarly purposes. Any copying or use of the material in this thesis for financial gain shall not be allowed without my written permission.

Signature Daniel L. Sutliff

Date July 27, 1989

DESIGN OF A LASER WELDING NOZZLE INCORPORATING AN AERODYNAMIC WINDOW FOR LASER BEAM DELIVERY OPTICS PROTECTION

A Thesis

Presented for the

Master of Science

Degree

University of Tennessee, Knoxville

Daniel L. Sutliff

August 1989

This work is dedicated to my lovely bride, Linda.

ACKNOWLEDGEMENTS

The author wishes to express his appreciation to Dr. T.D. McCay and Dr. M.H. McCay for their guidance and encouragement in completing this work. Appreciation is also extended to C.M. Sharp and the entire staff and students at the University of Tennessee Space Institute (UTSI) Center for Laser Applications (CLA). Without their technical assistance this thesis could not have been done. Special thanks to Rick Neal for typing the Thesis.

This work was done at the University of Tennessee Space Institute Center for Laser Applications during the period from September 1988 to August 1989.

ABSTRACT

Lasers used for welding contain a series of reflective and transmission optics which if not kept free of contamination results in aberrations in the laser beam and subsequent degradation in the properties of the weld. Downtime is necessary to clean the optics and maintain the weld quality. Particle build-up on the optics may even cause physical damage such as fracture, necessitating replacement with its attendant material costs. Welding of aluminum alloys has been particularly damaging to the optics due to the presence of alloying elements, such as magnesium and manganese, which vaporize and deposit ejecta particles on the optics.

A welding nozzle with an aerodynamic window was developed to protect the laser beam delivery optics by preventing ejecta particles from depositing on the optics. The area and magnitude of the cross-flow through the window was optimized in a cold flow experiment with the nozzle removed from the laser. A series of welds were conducted with the cross-flow nozzle and the existing baseline laser welding nozzle. The degradation of power to the workpiece, particle distribution on the reflective optics and integrity of the Zn-Se transmission optic was noted. The weld structure was examined to ensure that there was

no interference with the quality of the weld due to the cross-flow.

The aerodynamic window substantially reduced the amount of particle build-up on the reflective optics. Loss in the power delivered to the workpiece was reduced. During the baseline nozzle experiments the Zn-Se optic was destroyed, while during the cross-flow nozzle experiments the optic remained intact. The ratio of deep penetration to conduction limited weld was greater and the percentage porosity was lower for the cross-flow nozzle welds. Comparison of weld penetration and depth-to-width ratio of the welds showed little difference between the two nozzles.

TABLE OF CONTENTS

LIST OF FIGURES

I. INTRODUCTION

ALUMINUM LASER WELDING

Laser Beam Welding uses a high-power monochromatic light beam focused on the material to be welded. The material absorbs a portion of the laser beam energy resulting in the formation of a keyhole which as the workpiece is moved produces a deep penetration weld. A plasma is formed when the workpiece material evaporates and ionizes in the keyhole region. The keyhole provides a surface through which heat is transferred to the bulk of the material. Molten material flows around the keyhole and solidifies, forming the weld. A stable keyhole and plasma will result in a desirable deep penetration weld, characterized by cross-section depth to width ratios of unity and greater. Destabilization of these properties may result in a conduction limited weld, whereby there is no keyhole formation and the only heat transfer mechanism is conduction through the material. Conduction limited weld cross-section depth-to-width ratios are typically one-half to one or less.

The laser welding of aluminum has been difficult due to the inherent characteristics of the material: High thermal conductivity, (about two to four times that of mild steel), high electrical conductivity, (about three to five times that of mild steel), low melting point (about 500 to 600°C), low strengths at elevated temperatures and the presence of natural oxidizing layers. Specific aluminum alloys have additional laser welding difficulties due to the alloying elements which vaporize during the welding process. The vaporization of the alloying elements can carry with it ejecta particles. A portion of the vaporized gasses and ejecta is shot up through the laser nozzle and is deposited on the laser beam delivery optics and mirrors. This contamination can degrade the quality of the laser beam, causing loss in the power delivered to the workpiece, variations in the quality of the weld, and may eventually result in fracture of the Zn-Se window in the welding nozzle assembly. The loss in power delivered to the work piece necessitates downtime in order to restore the efficiency by cleaning the mirrors. Variability in the weld affects the quality control in a manufacturing process and has made meaningful parametric studies of aluminum laser welds impossible. Fracture of the Zn-Se window, in addition to the expense associated with the downtime, will have the additional material cost of replacing the window.

UTSI CLA LASER DESCRIPTION

The laser used for this study was a Rofin-Sinar model RS 3000 RF excited, fast axial flow industrial CO_2 laser. The laser power output can be continuously varied between 0.2 and 3.7 kilowatts. The laser can be configured to run in three different spatial modes:

1. TEM_{00};
2. TEM_{01};
3. TEM_{10};

In addition, four temporal modes can be selected:

1. C.W. (Continuous Wave);
2. Quasi CW (Pulse Width Modulated at 5kHz);
3. Gated Pulse (up to 25 kHz);
4. Superpulsed (up to 25 kHz).

The manipulation of the workpiece is achieved with a five axis CNC computer driven Aerotech workstation. A schematic of the laser beam delivery system is shown in figure 1. The transmission optic is a Zn-Se window and the reflective optics are a flat, molybdenum coated

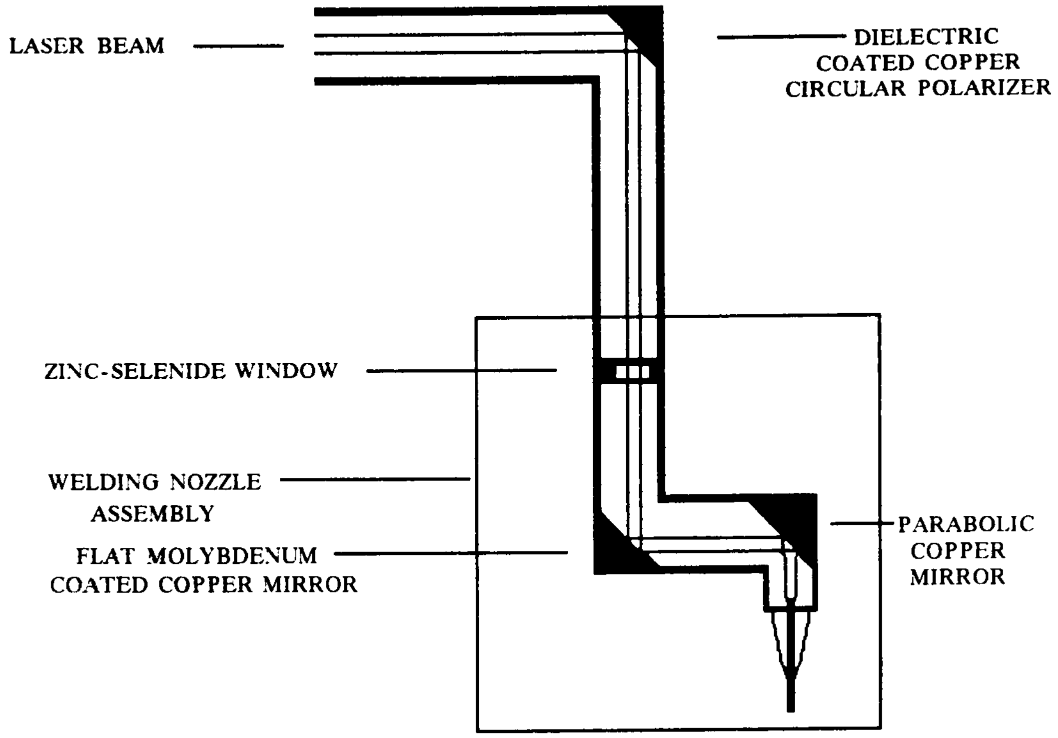

FIGURE 1. UTSI CLA Laser Beam Delivery Optics.

copper mirror and a parabolic copper mirror. The parabolic mirror, being in a direct line above the workpiece, is most often contaminated by ejecta particles, while the Zn-Se window being at the top of a the nozzle assembly is most affected by the rising vaporized metal.

EXISTING BASELINE NOZZLE FOR LASER WELDING

The nozzle currently in use at the UTSI CLA for laser welding is cone shaped, with two gas jet inputs, a co-axial, and a side gas jet flow. The existing baseline nozzle is shown in figure 2. The co-axial gas jet flow shields the weld area with a non-oxidizing gas, typically argon or helium. A typical flow rate for the co-axial gas jet is 5.7 l/min. The side gas jet flow is used for plasma control and settings vary depending on the material being welded.

AERODYNAMIC WINDOWS

Aerodynamic windows have been used with lasers since the introduction of the first high energy laser, the Gas Dynamic Laser (GDL). An aerodynamic window consists of a cross-flow of pressurized gas flowing nearly perpendicular to the beam propagation. This cross-flow

- dimensions in cm
- material : copper

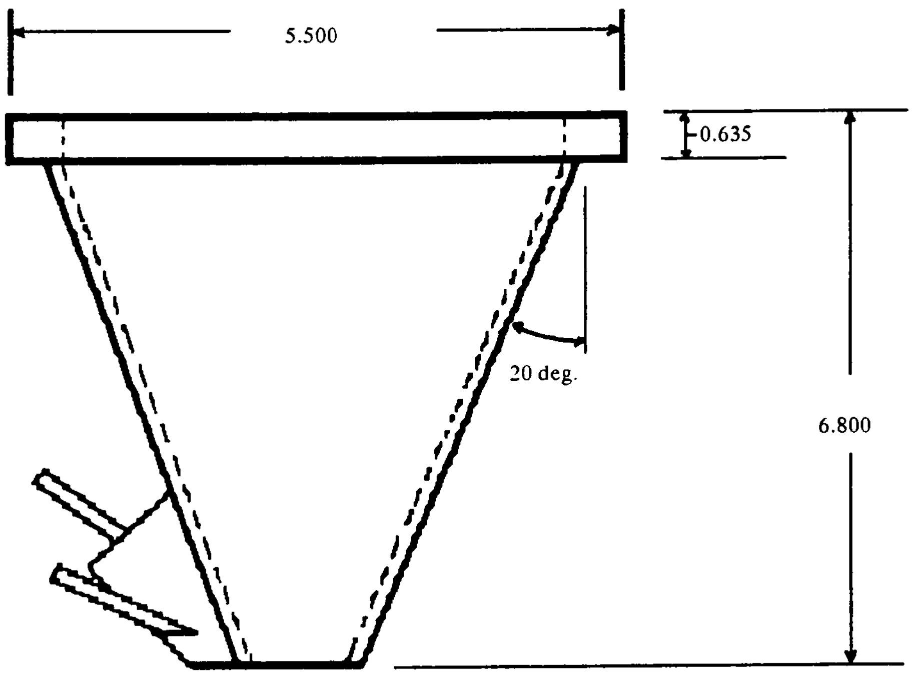

FIGURE 2. Existing UTSI CLA Baseline Laser Welding Nozzle Tip.

is usually supersonic, but a few are subsonic. The purpose of existing aerodynamic windows is to maintain the gas and the desired pressure within the laser cavity (while still optically transmitting the beam) by providing a pressure barrier between ambient and the laser beam cavity. A review of the literature did not find any examples of an aerodynamic window used in the nozzle area to protect the laser optics. The purpose of this study is to develop such an aerodynamic window.

II. NOZZLE CONCEPTUAL DESIGN

NUMERICAL ANALYSIS

The first order equations of motion were applied to calculate the dimensions of the aerodynamic window and the amount of required cross flow. The equations of motion are:

1) $F = C_d A 1/2 \rho V^2$

2) $F = m(-a)$

Where:

F	Drag Force on Particle;
C_d	Drag Coefficient;
A	Particle Frontal Area;
ρ	Density of Air;
V	Relative Velocity between Cross-flow and Particle;
m	Mass of Particle;
a	Deceleration of Particle Due to Drag.

These equations were solved with a forward time marching solution to estimate the trajectory of a particle entering the cross-flow. From video tape recordings of previous weld experiments, the ejected particles were assumed to be spherical, 0.1 mm in diameter with a velocity of 7 m/sec. The drag coefficient, C_d, was assumed to be that of a sphere in incompressible, inviscid flow. The nominal particle size and velocity were bracketed and the equations solved for different cross-flow velocities. From figure 2, it was estimated that a particle would have to travel about 2 cm horizontally before travelling 3 cm vertically to prevent the particle from striking the mirror. This estimate, superimposed with the results of the numerical studies in figure 3, shows that a cross-flow of about 10 to 20 m/sec would satisfy this criteria.

The cross-flow is more effective in removing smaller particles. This is due to the fact that the force required to alter the trajectory is proportional to the diameter cubed, while the altering force, drag, is proportional to the diameter squared. However, since the numerical studies suggest that the cross-flow is more effective on particles with smaller entry velocities, the cross-flow should be equally efficient in removing particles more massive, slower moving particles.

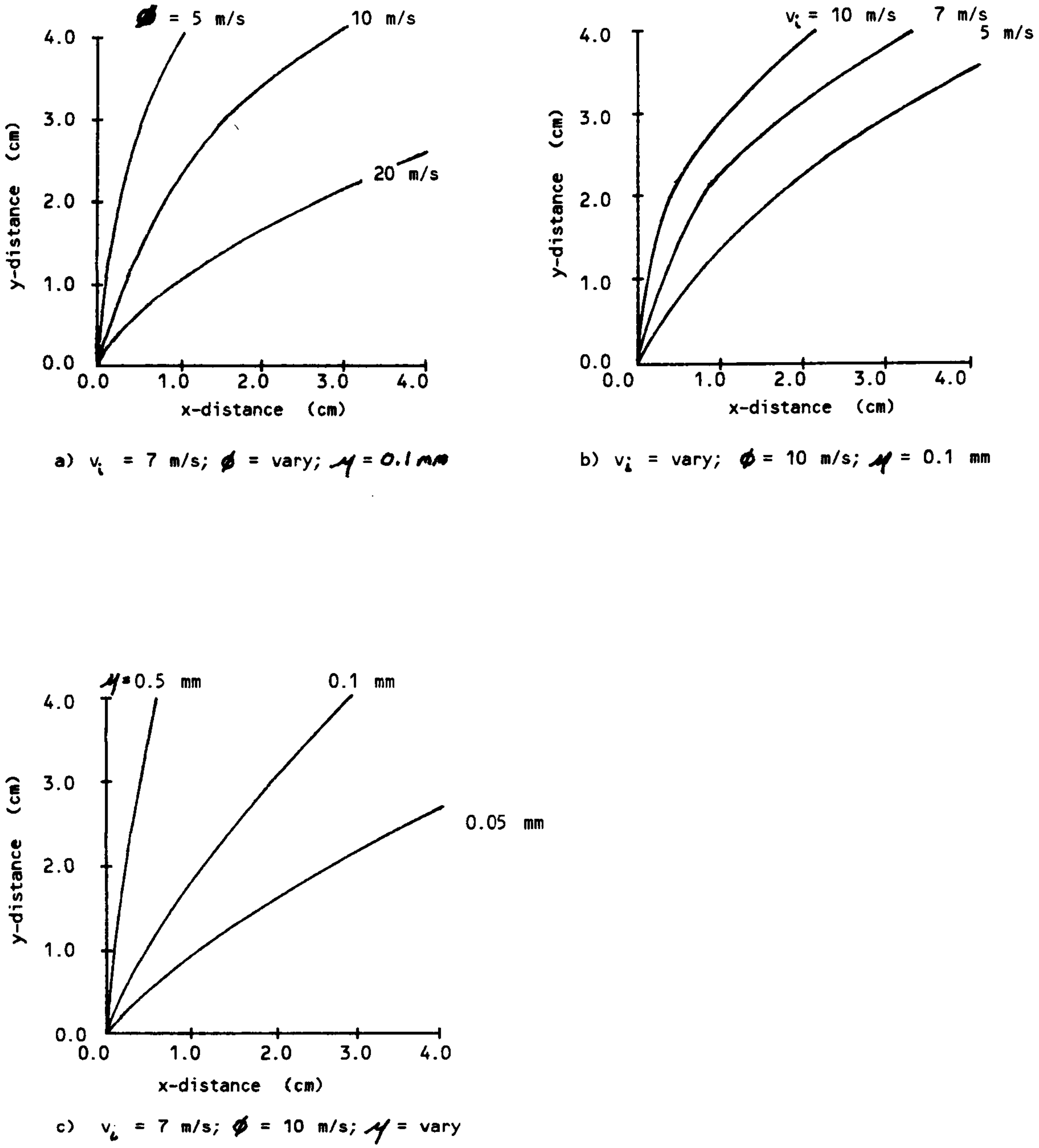

FIGURE 3. Numerical Estimate of Particle Trajectory in Cross-Flow: v_i, initial particle velocity in y-direction; ϕ, cross-flow velocity in x-direction; d, particle diameter.

NOZZLE DESIGN

A nozzle was designed based on dimensional constraints from the existing laser focusing assembly. The nozzle is comprised of four sections to facilitate development changes and for ease of fabrication. The four sections, shown in figure 4, are the cross-flow inlet tunnel, cross-flow exhaust tunnel, cylindrical base, and conical tip. The inlet tunnel contains a 0.5 square mm wire screen mesh to straighten the cross-flow and minimize dead spots. Design of the cross-flow inlet as a separate piece allows for the insertion of shims to optimize the area/velocity parameters of the cross-flow. The assembled nozzle is shown in figure 5. A co-axial gas jet flow tube was inserted as in the existing nozzle to prevent oxidation of the workpiece.

COLD FLOW EXPERIMENTS

An experiment was designed to examine the ability of the cross-flow jet to remove particles from the nozzle interior (figure 6). For the particle feed system, a hopper is filled with sand blasting particles with a density of 1.5 kg/l and an average size of 0.5 mm in diameter (which compares favorably to the estimated size of ejecta particles). The hopper is back pressurized to assist gravity in the feed of the

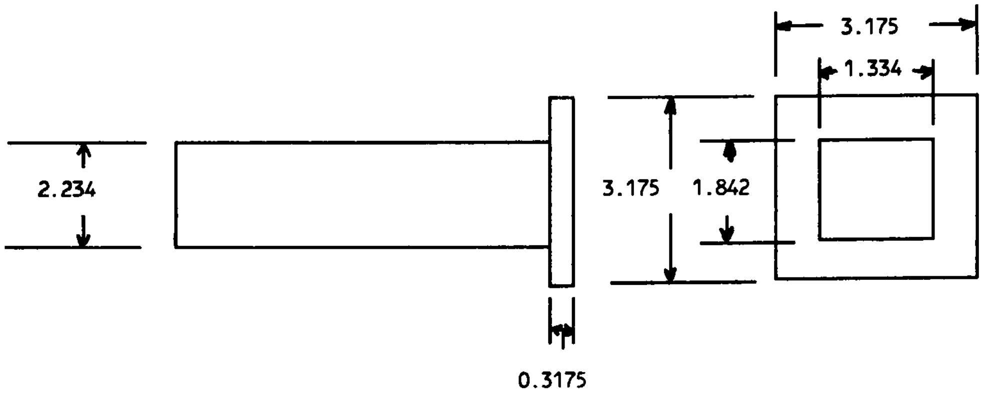

Inlet tunnel has mounting plate
for 1/4" tubing and 0.5 mm square
wire mesh for flow straightening.

a) Inlet and Exhaust Flow Tunnels.

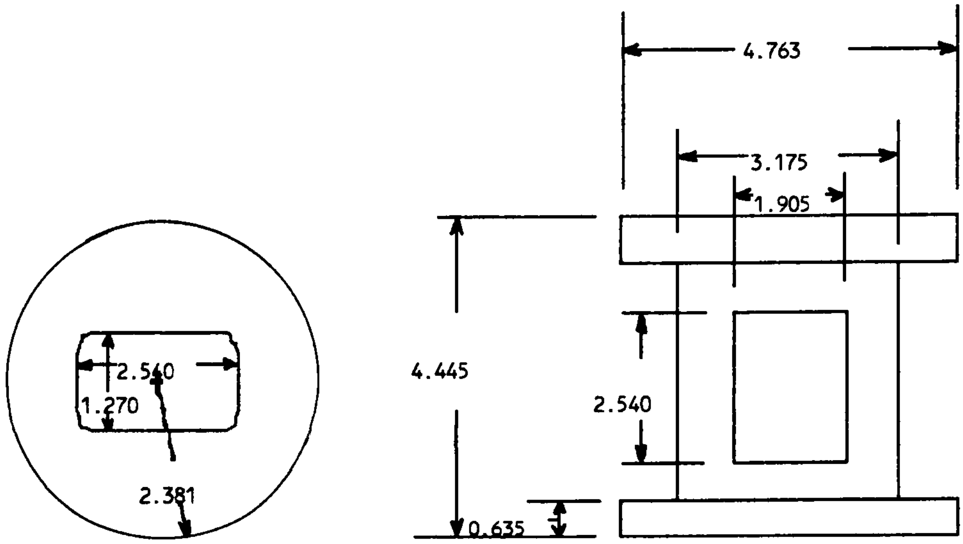

b) Cylindrical Base.

- dimensions in cm
- material : copper

FIGURE 4. Cross Flow Nozzle Components.

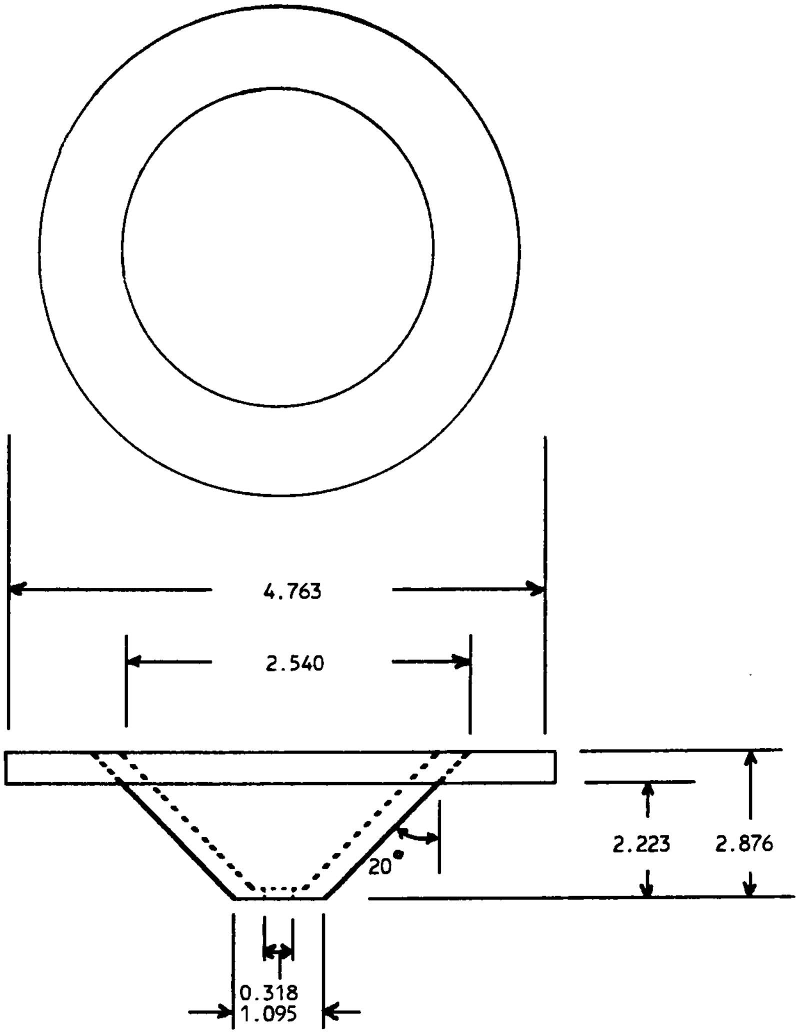

- dimensions in cm
- material : copper

c) Conical Tip.

FIGURE 4. Continued.

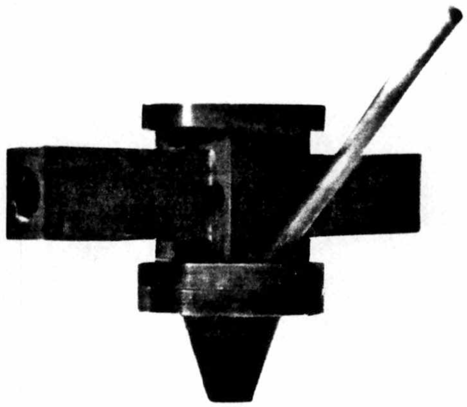

FIGURE 5. Assembled Cross-Flow Nozzle.

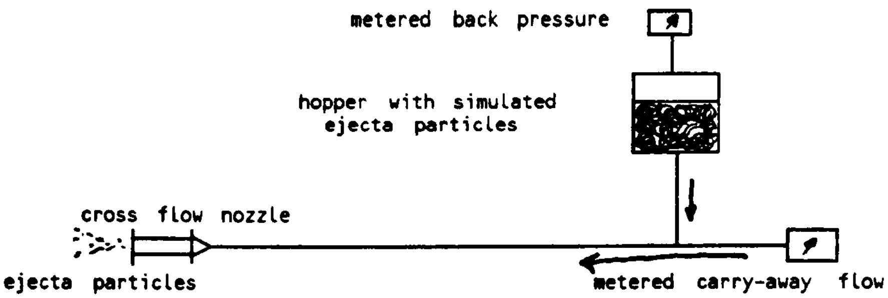

a) Particle Feed System.

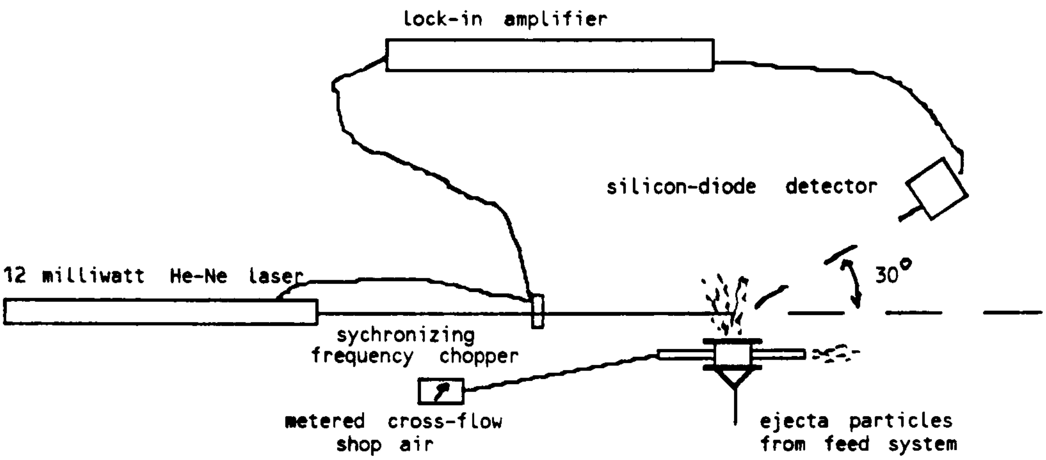

b) Measurement System.

FIGURE 6. Cold Flow Experimental Schematic

particles. The base of the hopper is connected by tubing to the base of the nozzle tip. The particles are fed into the airflow and the interior of the nozzle through this tubing. In the measurement system, pressurized shop air is fed into the cross flow inlet tunnel. A 12 milliwatt Helium-Neon laser is focused across the top exit of the cylindrical base. A Silicon diode detector electrically connected to a lock in amplifier is set at approximately a 30 degree angle from the beam travel. The laser and the amplifier are synchronized by a frequency chopper set at 186 Hertz. Particles exiting from the cylindrical base scatter the laser beam and the portion of the beam deflected 30 degrees is measured by the Silicon diode detector.

Since not all of the particles deflect the beam exactly onto the Silicon diode detector, it was necessary to statistically calibrate the amplifier readings. To do this, the carry away flow and back pressure were varied for each run, with zero cross-flow. The feed was activated for a period of sixty seconds during which the intensity of the laser deflection from the particles coming out of the top of the nozzle was measured in volts from the amplifier reading. The mass of the material removed from the hopper was then measured. After refilling the hopper to the previously marked "full" level, the run was repeated at another carry away/back pressure setting. The resulting mass flows and intensities were normalized by their respective highest values and are plotted in figure 7. There is a linear relationship to the measured intensity of the laser deflected off of the particles and the mass flow (and number) of the particles. This technique is therefore a valid indicator of the number of particles exiting the cylindrical base.

The effectiveness of the cross-flow to prevent particles from exiting at the top of the cylindrical base was then measured. The cross-flow was increased from 0 to 208 l/min, which was the maximum amount available from the shop air supply. The run was repeated for carry away/back pressure settings of 4.4/4.4, 7.6/4.4 and 11.3/7.6 l/min. These represent different particle entry velocities. The matrix was repeated for three different window areas by placing shims between the inlet tunnel and nozzle base. The three windows were; full (area = 2.46 cm), half-horizontal (1.23 cm), and half-vertical (1.23 cm). The intensity of the deflected laser beam at a given cross flow setting was normalized to the intensity at zero cross-flow and plotted versus cross flow in figure 8 for each window at various carry away/back flow

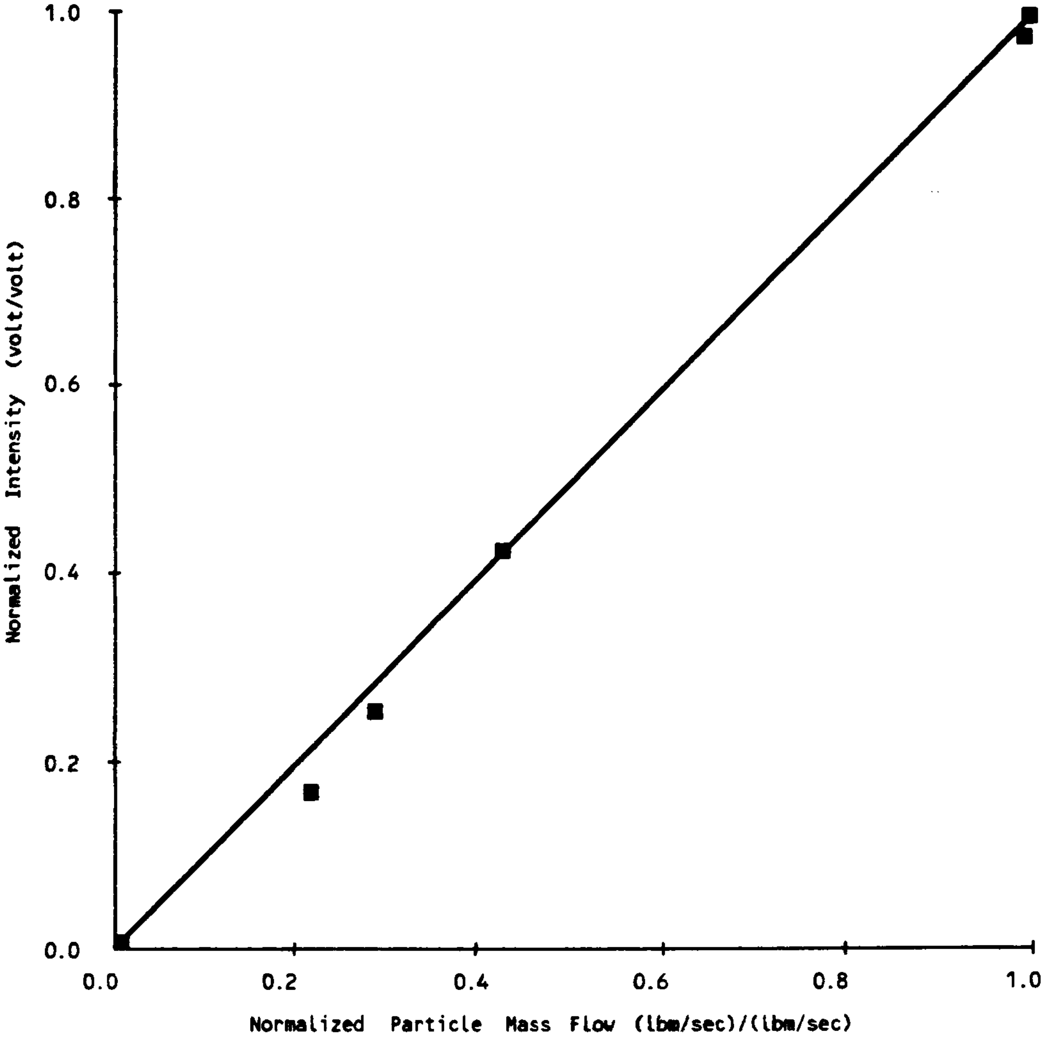

FIGURE 7. Intensity of Deflected Laser Beam as a Function of Particle Mass Flow (normalized to highest reading).

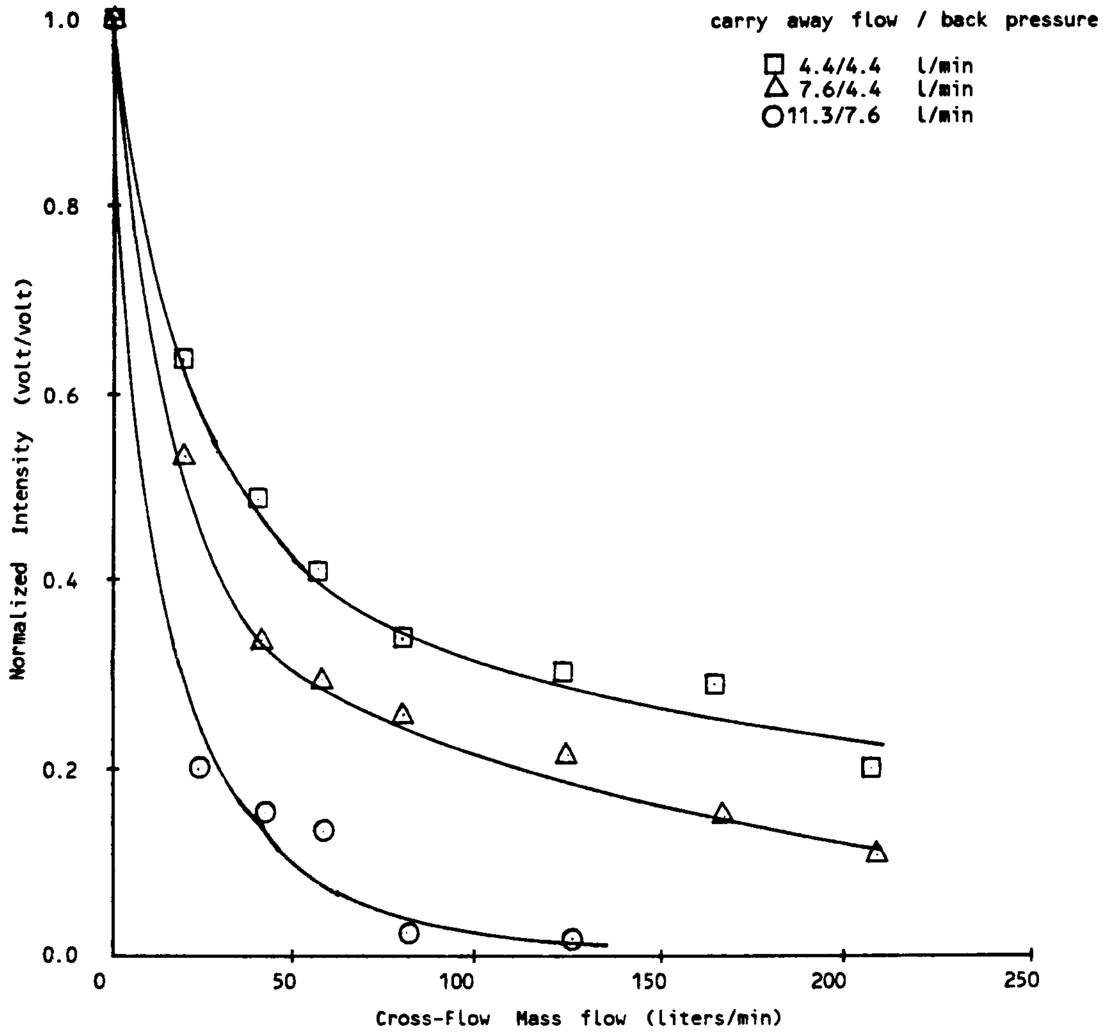

a) Normalized Intensity of Deflected Laser Beam as a Function of Cross-Flow. Full Window (area = 2.46 cm^2).

FIGURE 8. Cold Flow Experiment. Cross Flow Effectiveness.

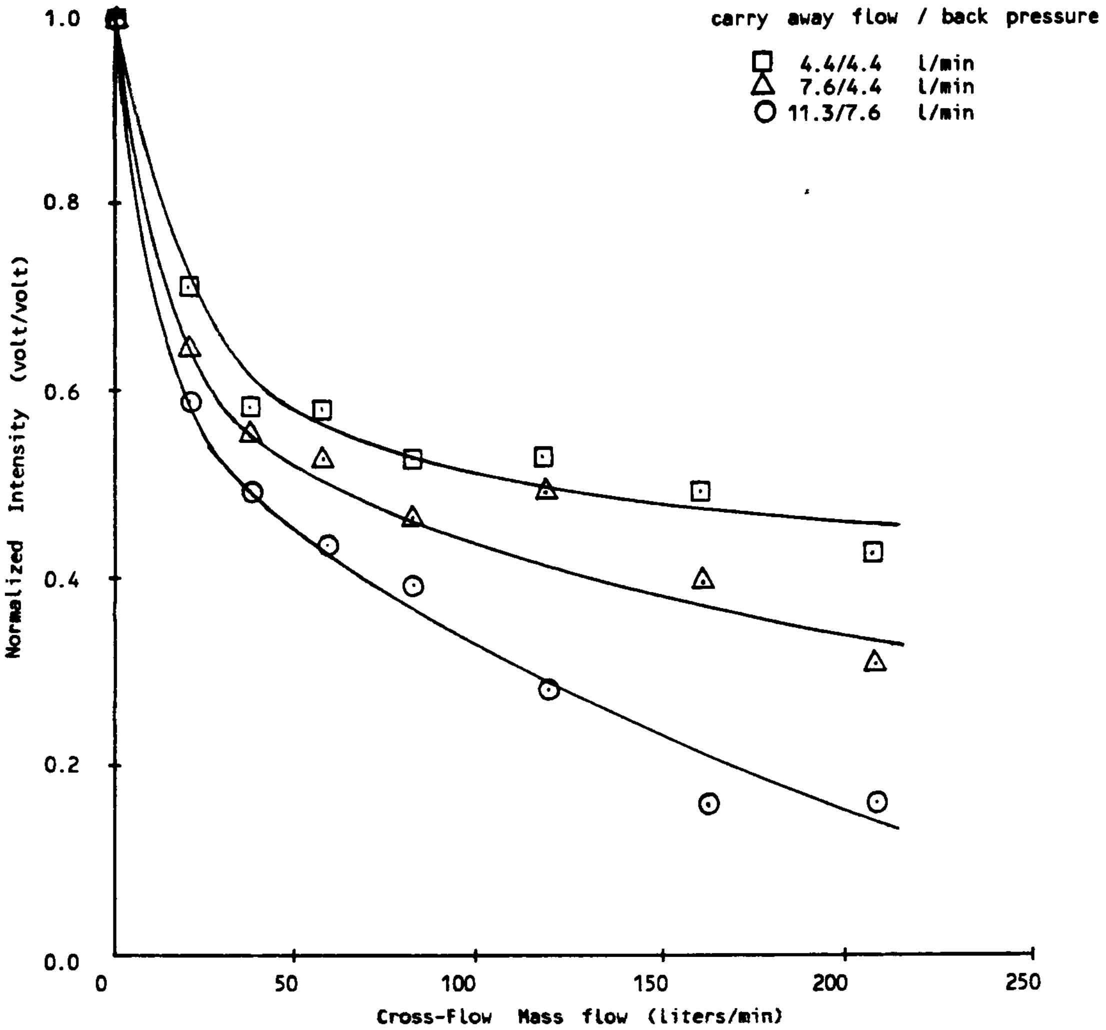

b) Normalized Intensity of Deflected Laser Beam as a Function of Cross-Flow. Horizontal Half Window (area = 1.23 cm^2).

FIGURE 8. Continued.

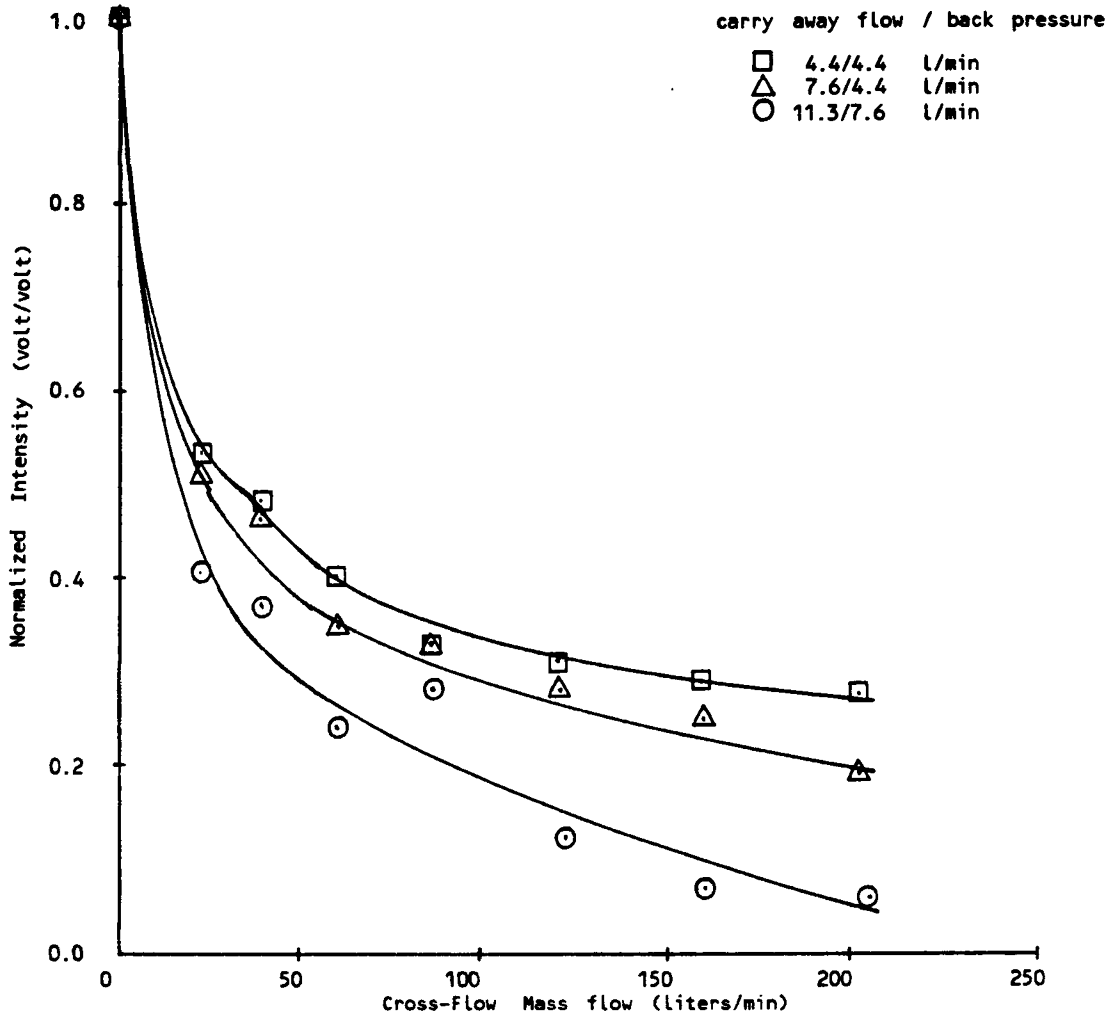

c) Normalized Intensity of Deflected Laser Beam as a Function of Cross-Flow. Vertical Half Window (area = 1.23 cm^2).

FIGURE 8. Concluded.

pressures. The results show that the full window (area = 2.64 cm) is the most efficient and that while increased cross flow would most likely improve the particle removal, the data are near the point of diminishing returns. The shop air maximum flow rate (208 l/min) combined with the optimum area gives a flow velocity of 14 m/sec through the window.

The nozzle was also tested to see if the cross flow-jet had any fluid dynamic effect on the nozzle tip. A flow meter was connected to measure any inflow or outflow from the nozzle tip. The cross-flow was set to two values, 0 and 208 l/min. The cross-flow caused no measurable inflow or outflow at the nozzle tip.

III. LASER WELD STUDY

METHODOLOGY

Aluminum alloy 5052 was chosen because the concentration of magnesium and manganese are thought to be the cause of ejecta related problems during laser welding. The composition is shown in table 1. The weld parameters are shown in table 2. Square plates, 200x200x6 mm were sand blasted to a visibly smooth surface then welded bead on plate in a series of runs. The path of the weld was a square shape, with the perimeter decreasing in toward the center of the plate. The power delivered to the workpiece by the laser was measured by a Scientech 39-0201 Water Cooled Calorimeter after each square length of weld. To accomplish this, the beam is directed into the calorimeter. Through a series of reflections, the beam is completely absorbed and converted into heat. The heat causes a temperature rise in the water passing through the heat exchanger, which is a measure of the power being dissipated in the calorimeter.

The intention was to fill the surface of the plate with welds, decreasing the square path in toward the center of the plate. The baseline nozzle was used first. During the studies, while measuring the power output

TABLE I. 5052 Composition.

Element	% WT
Al	remainder
Cu	0.10
Mn	0.10
Mg	2.50
Cr	0.25
Zn	0.20

TABLE II. Welding Parameters.

Parameter	Setting
laser power	3 kW
laser mode	TEM_{01}
laser temporal mode	CW
co-flow input	5.7 l/min
co-flow output	0 l/min
weld speed	40 mm/sec
focus depth	1 or 2 mm

(after 2800 mm or 40% of the weld length) the Zn-Se window was found to be cracked. Upon examination, the cracked window was seen to be coated with a very fine layer of particle dust. It is hypothesized that the minute particles from the ejecta, being able to travel further due to their lighter size, were deposited on the surface of the Zn-Se window. This coating prevented the window from fully transmitting the laser beam and the resulting absorption of energy by the window caused it to crack. Further studies with the baseline nozzle were terminated out of concern for destroying another Zn-Se window.

During the cross-flow nozzle studies 7000 mm of weld were made with the cross-flow set to 208 l/min. No problems were encountered.

The experiment to determine if there were any cross-flow/co-axial flow interactions was repeated with the assembly on the laser. Again, there was no measurable effect on the flow at the nozzle tip between cross-flow off or cross-flow on (208 l/min), with no co-axial flow. This time, however, an additional effect was investigated. A co-axial gas jet flow of 17.0 l/min was set and the outflow from the nozzle tip was measured. Only 0.04 l/min of the input co-axial flow was measured coming out at the nozzle tip, the remainder flowed out the cross-flow exhaust tunnel. Due to the path of lesser fluid resistance offered by the large exhaust tunnel opening (relative to the nozzle tip exit) this result was independent of the cross-flow setting. As a result of this effect, the composition of the shielding gas for the cross-flow nozzle welds is unknown. It is thought that it is almost entirely an air weld.

ANALYSIS OF RESULTS

The power delivered to the workpiece by the laser beam was measured with cleaned and polished mirrors prior to welding and after selected runs. The power delivered to the workpiece was divided by the power input to the laser to get an efficiency. This ratio was then normalized by the pre-welding delivery efficiency. The normalized efficiency vs. the weld length is shown in figure 9. After equal lengths of welds (2800 mm) the normalized efficiency of the baseline nozzle was 71.0% compared to 96.4% for the cross-flow nozzle, a 36% improvement. After the full length of welds with the cross-flow nozzle (7000 mm), the normalized efficiency was 88.6%. Extrapolating the cross-flow nozzle data to the 71.0% efficiency would give a weld length of 17,800

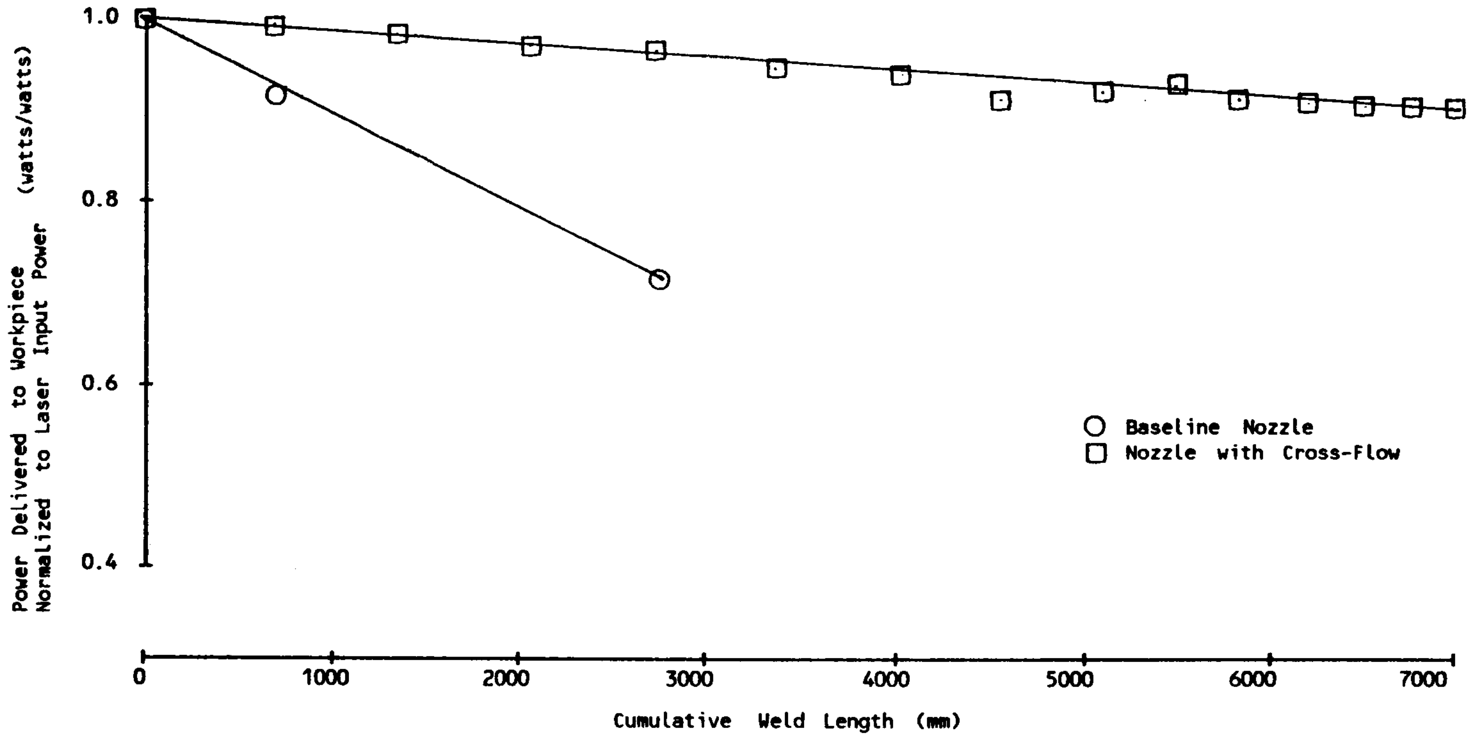

FIGURE 9. Efficiency of Laser Power Delivered to Workpiece as a Function of Cumulative Weld Length.

mm, a factor of 6.4 weld length improvement over the baseline nozzle.

After the welds were completed for a nozzle case the parabolic mirror was removed. The particles deposited on the mirror were collected with clear adhesive tape, examined under 8x magnification, and measured. Particles deposited on the mirror tend to assume a flat oval shape and were measured as such. The distribution of the number of particles having a given area was recorded. To account for the different weld lengths the area distribution was normalized by the total weld length. The results of the particle distribution analysis is shown in figure 10. The cross-flow nozzle removed approximately 80% of the smaller particles (less than .2 mm^2) and all of the larger particles (larger than .2 mm^2) when compared to the baseline nozzle.

Analysis of the weld character also shows differences between the two nozzles. A binary plot (deep penetration = 1, conduction limited = 0) of the weld type is given in figure 11. The baseline nozzle started with a deep penetration weld, then destabilized to a conduction limited weld. The length of conduction limited weld per perimeter weld increased with

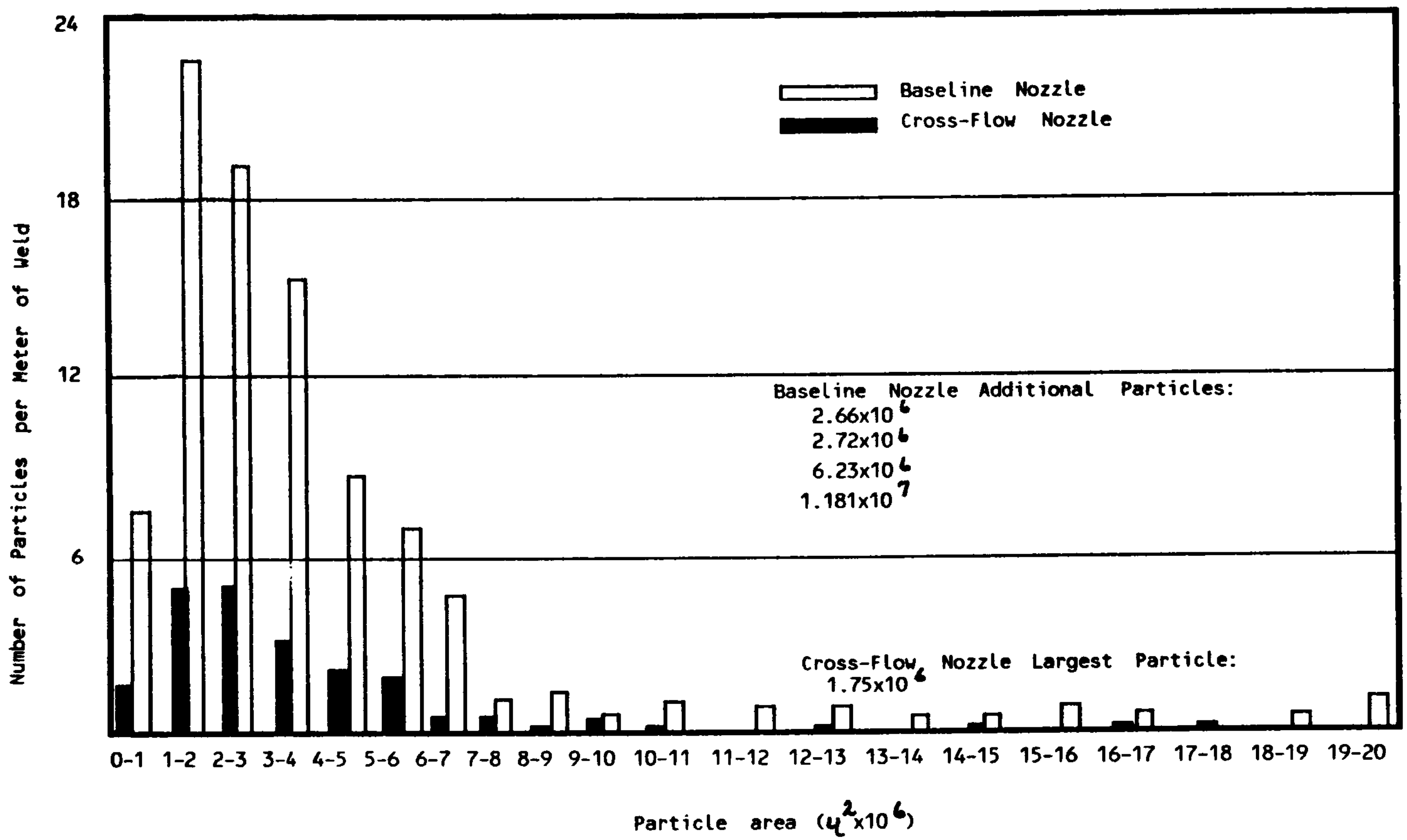

FIGURE 10. Area Distribution of Particles Deposited on Mirror per Meter of Weld.

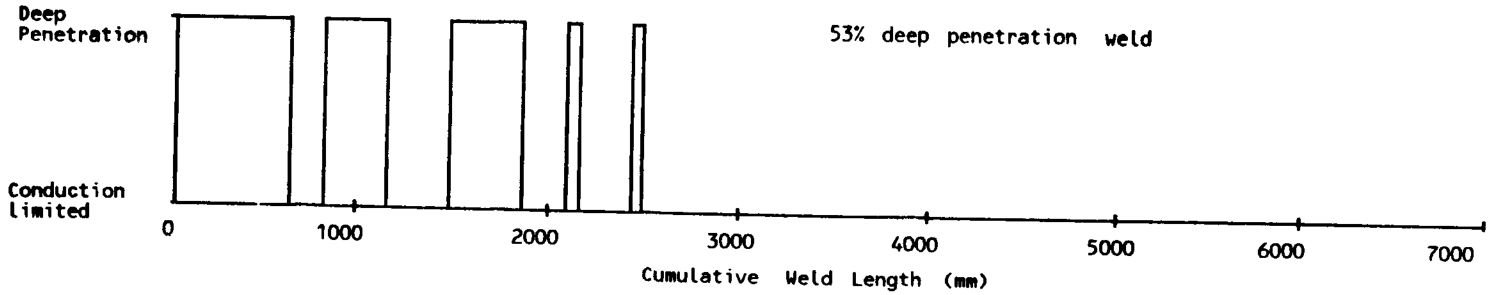

a) Baseline Nozzle.

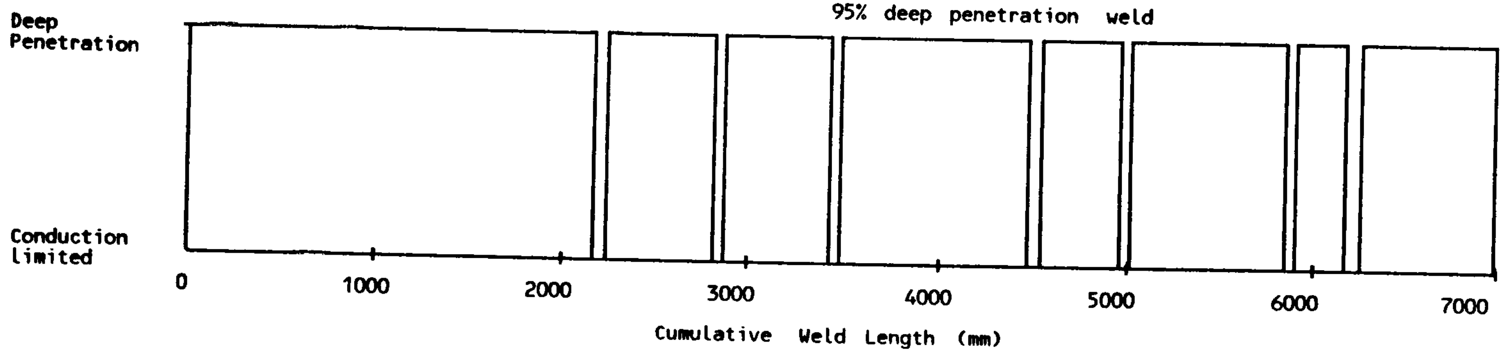

b) Nozzle with Cross-Flow.

FIGURE 11. Type of Weld as a Function of Cumulative Weld Length

increasing total weld length. The overall deep penetration to conduction limited weld ratio was 53%. It is felt that the destabilization of the weld was due to the instabilities in the beam caused by the optics degradation.

Inspection of the surface cross-flow nozzle welds showed 95% were deep penetration. However, in this case, the weld would start in the conduction limited mode, then restabilize to a deep penetration weld. It was determined that ash and condensed metal vapor build-up at the tip of the nozzle was interfering with the laser beam. After a short distance the beam would burn through the build-up and a deep penetration weld continued for the remainder of the weld. Proper cleaning of the nozzle tip with a wire brush prior to welding, eliminated the conduction limited weld start.

The welded plates were cross-sectioned, mounted and polished. The cross sections were analyzed for depth of penetration, depth-to-width ratio and porosity. Figure 12 shows the measured depth of penetration of the weld. The average penetration depth is approximately the same for the two nozzles, however, the cross-flow nozzle exhibits less variation. No trend with weld length is apparent. Figure 13 shows the

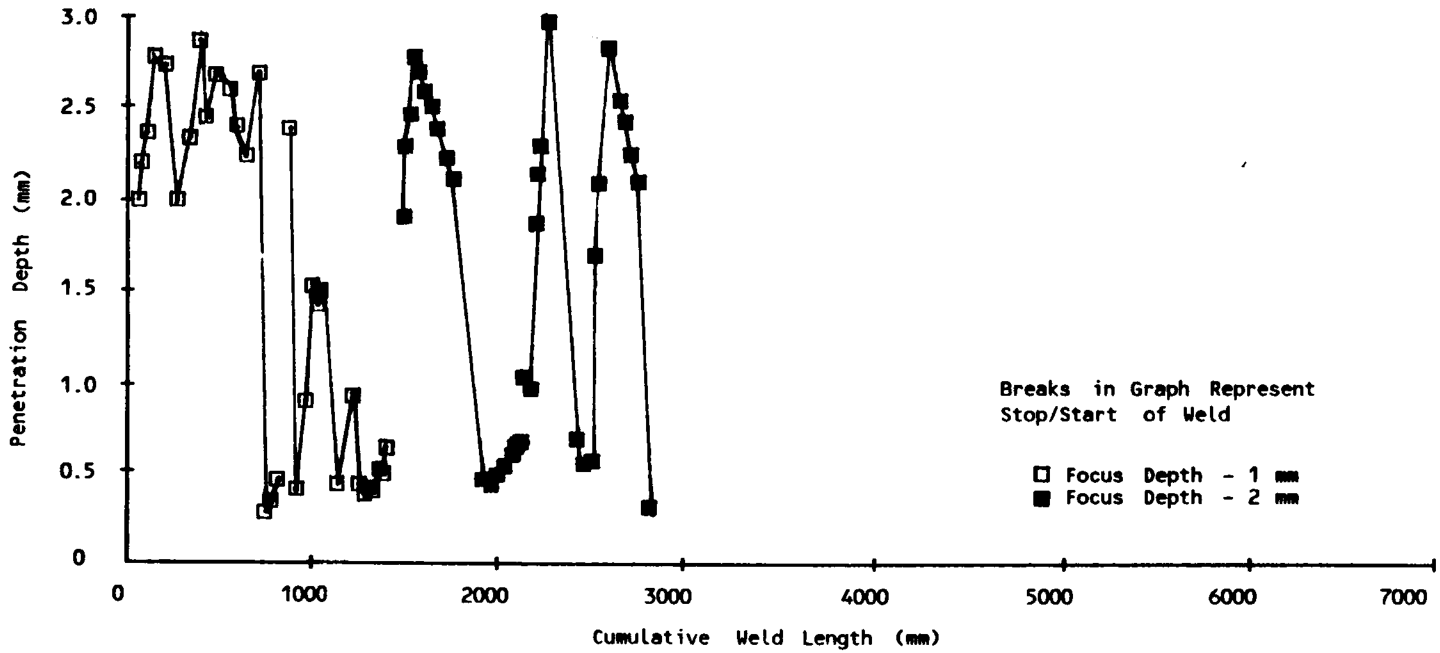

a) Weld Penetration Depth as a Function of Cumulative Weld Length for Baseline Nozzle. (Zn-Se Window Cracked after 2800 mm of Weld).

FIGURE 12. Weld Penetration Depth.

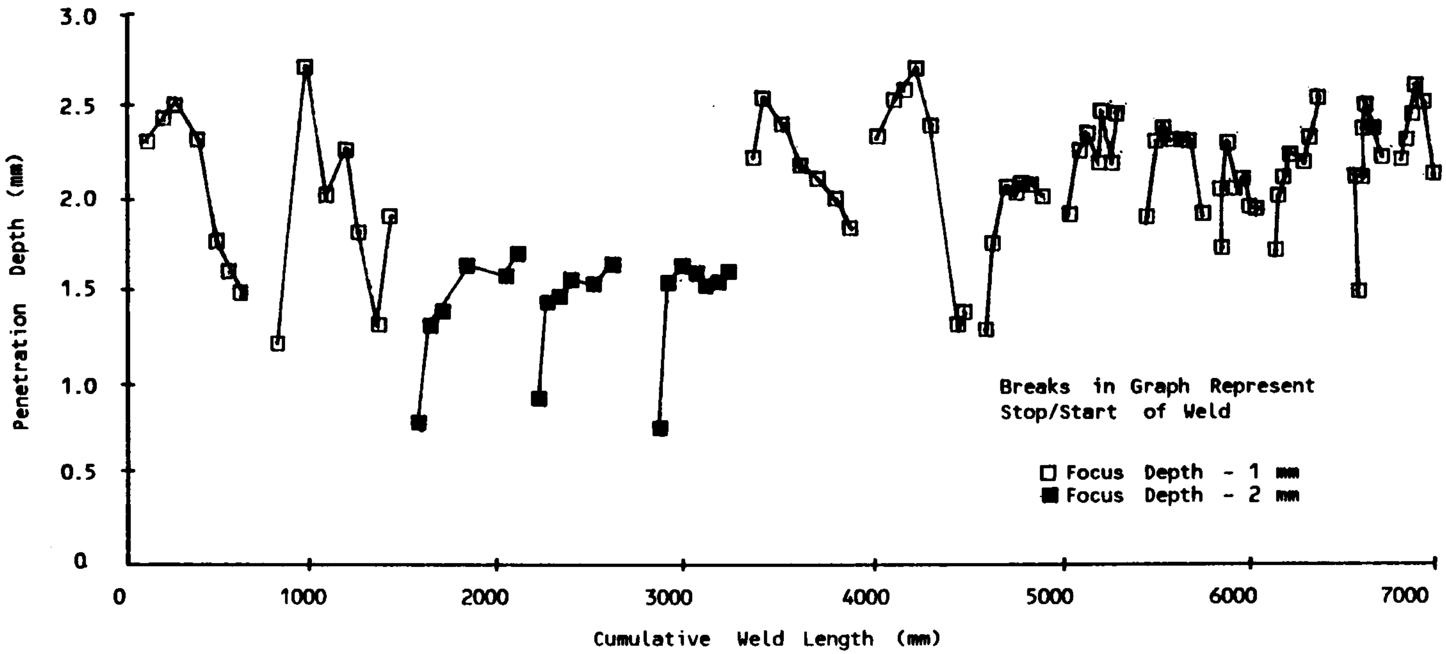

b) Weld Penetration Depth as a Function of Cumulative Weld Length for Cross-Flow Nozzle.

FIGURE 12. Continued.

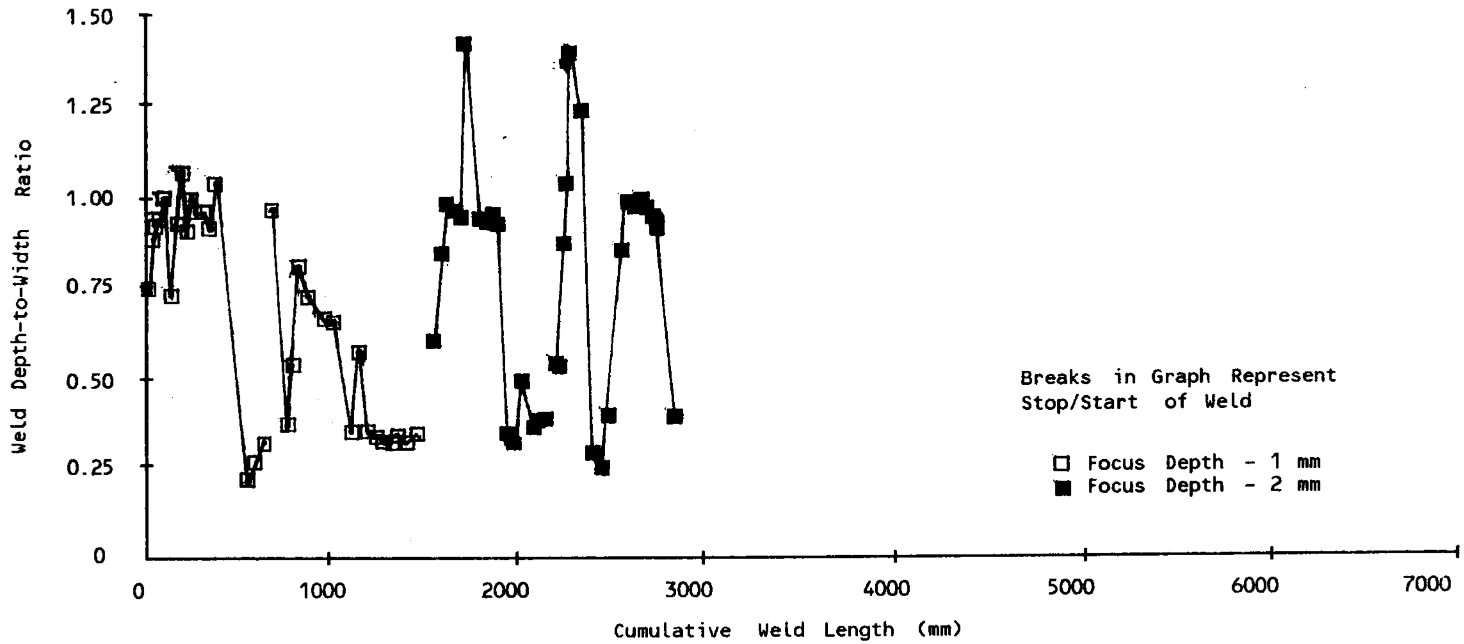

a) Weld Depth-to-Width Ratio as a Function of Cumulative Weld Length for Baseline Nozzle. (Zn-Se Window Cracked after 2800 mm of Weld).

FIGURE 13. Weld Depth to Width Ratio.

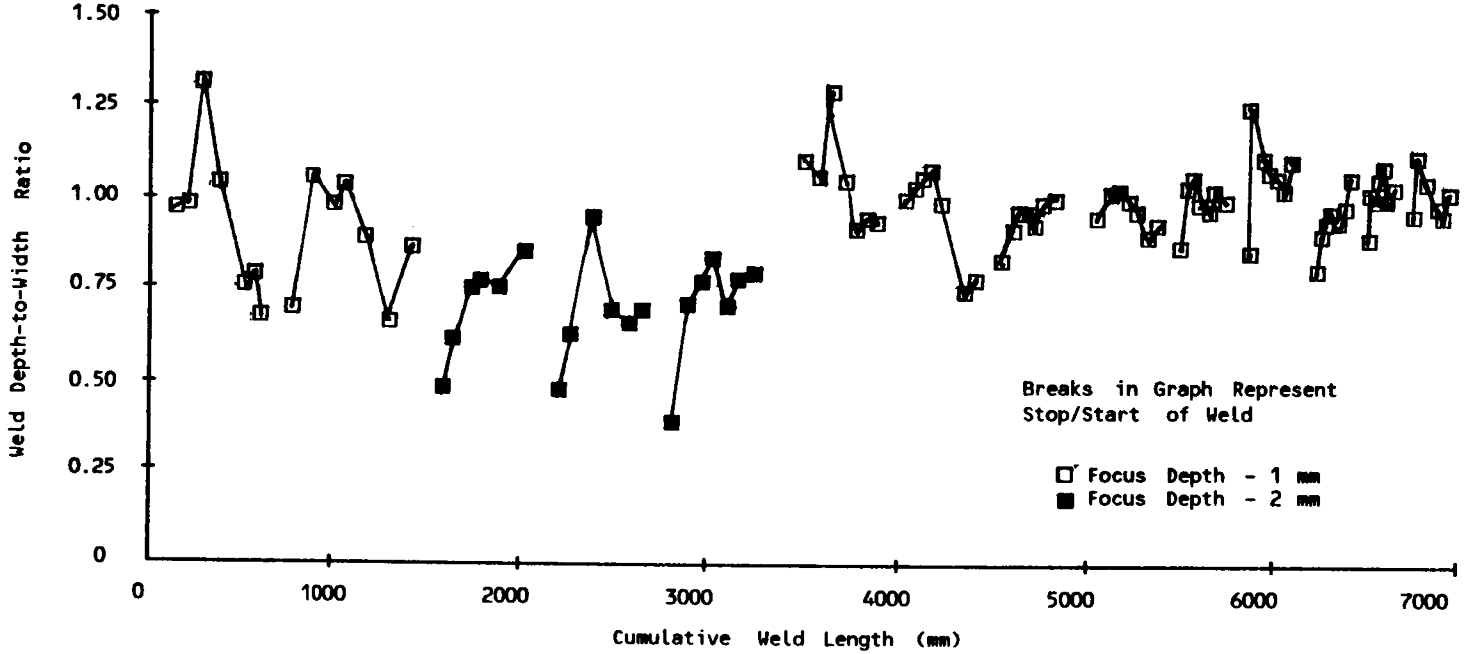

b) Weld Depth-to-Width Ratio as a Function of Cumulative Weld Length for Cross-Flow Nozzle.

FIGURE 13. Continued.

depth-to-width ratio of the weld. The observations for depth to width are similar to those mentioned for the deep penetration depth. The area of the porosity in the cross-section of the weld is shown in figure 14. The cross-flow nozzle weld cross sections tended to have several very small porosities (e.g. 4-6 on the order of $10^3\mu^2$). The average porosity for the cross-flow nozzle was 2.0%. The baseline nozzle tended to have a single, large porosity (on the order of $10^5\mu^5$), with an average porosity area of 17%. However, the conclusion that the cross-flow is directly responsible for the differences in porosity cannot be firmly supported. The unknown composition of the shielding gas may be responsible.

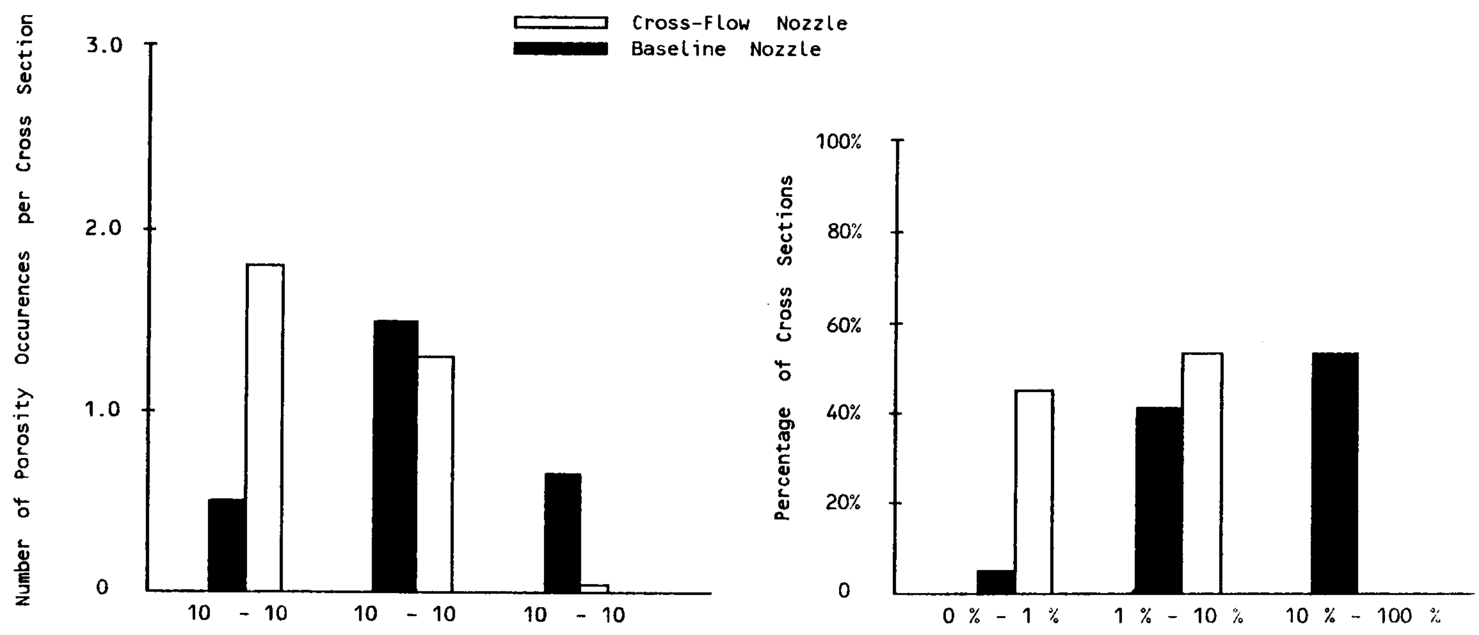

a) Porosity Area Distribution.

b) Percentage of Cross Sections with a Given Percentage Porosity.

FIGURE 14. Porosity of Weld Cross Sections.

IV. SUMMARY AND RECOMMENDATIONS

The cross-flow nozzle is effective in protecting the reflective and transmission optics in the welding nozzle assembly. The Zn-Se optic remained intact throughout the cross-flow nozzle experiments for 7000 mm of weld length, while it was destroyed after 2800 mm of weld during the baseline nozzle experiments. Approximately 80% less ejecta particles were deposited on the parabolic mirror compared to the baseline nozzle for equivalent weld lengths. Based on the results of this study, the advantages to welding of the cross-flow nozzle are:

1) 36% reduction in power delivery degradation;
2) 80% greater deep penetration weld to total weld length ratio;
3) 6x increased weld length between reflective optics cleaning;
4) 88% less porosity by area in the weld.

Further studies are needed, such as an optimization study to see if lower cross flows result in similar performances. The ash build-up, which affected the weld starts should be investigated and eliminated. Primary consideration should be given to the determination and optimization of the shielding co-axial flow composition. The stabilization provided by the cross flow should allow for better parametric studies, which was one of the intents of the design.

BIBLIOGRAPHY

BIBLIOGRAPHY

Avidor J.M. "Improved Free-Vortex, Subsonic Aerodynamic Window," AIAA Journal, Vol. 17, November 1979.

Cole-Parmer Instrument Company, flowmeter Calibration Data Reference Curve Numbers, E80CT87, E7134.

Davis, M., etal, "Modeling the Fluid Flow in Laser Beam Welding," Welding Journal, July 1986.

Marsico, T.A. "Mass Transfer Studies of Aluminum Alloys 5083 and 7039," Pennsylvania State University Graduate School, M.S. Thesis, May 1988.

Mazumder, J., "Laser Welding: State of the Art Review," July 1982.

McCay M.H., etal, "Correlation of Plasma Characteristics with Weldment Properties for Laser Welded Aluminum Alloys," Center for Laser Applications, University of Tennessee Space Institute.

Parmantier, E.M. and Greenberg, R.A. "Supersonic Flow Aerodynamic Windows for High-Power Lasers," AIAA Journal, Vol. 11, July 1973.

Sharp, C.M. Private conversations from April to June 1989.

White, F.M. "Fluid Mechanics", McGraw Hill, New York, 1979.

Zysk, K.T. "Pulsed CO_2 Laser Welding of Inconel 718," University of Tennessee, M.S. Thesis, May 1988.

VITA

Daniel L. Sutliff was born in Youngstown, Ohio on July 27, 1962. He earned a Bachelor of Science in Aerospace Engineering in 1985 from the University of Cincinnati, Ohio. He was involved in research and testing in active boundary layer control at the David Taylor Naval Ship Research and Development Center in Bethesda, Maryland, in conjunction with the university's co-operative education program.

From 1985 to 1986 he was employed by McDonnell Douglas in Long Beach, California, doing stability and control development of advanced ultra high bypass engined transports. From 1986 to 1989 he was a Project Engineer in the Engine/Inlet Section for Calspan Corporation at the Arnold Engineering Development Center in Tullahoma, Tennessee. He supervised the preparation and conduct of wind tunnel tests and performed verification, analysis, and presentation of the final data package. Also during the same period, he worked toward his Master of Science in Aerospace Engineering at UTSI, obtaining it in August of 1989.

Mr. Sutliff will continue his graduate education with a Doctoral Fellowship at the University of Cincinnati starting in September of 1989.